The American Journal of Human Genetics, Volume *92*

Supplemental Data

Mutations in *DARS* Cause Hypomyelination with Brain Stem and Spinal Cord Involvement and Leg Spasticity

Ryan J. Taft, Adeline Vanderver, Richard J. Leventer, Stephen A. Damiani, Cas Simons, Sean M. Grimmond, David Miller, Johanna Schmidt, Paul J. Lockhart, Kate Pope, Kelin Ru, Joanna Crawford, Tena Rosser, Irenaeus F.M. de Coo, Monica Juneja, Ishwar C. Verma, Prab Prabhakar, Susan Blaser, Julian Raiman, Petra J.W. Pouwels, Marianna R. Bevova, Truus E.M. Abbink, Marjo S. van der Knaap, and Nicole I. Wolf

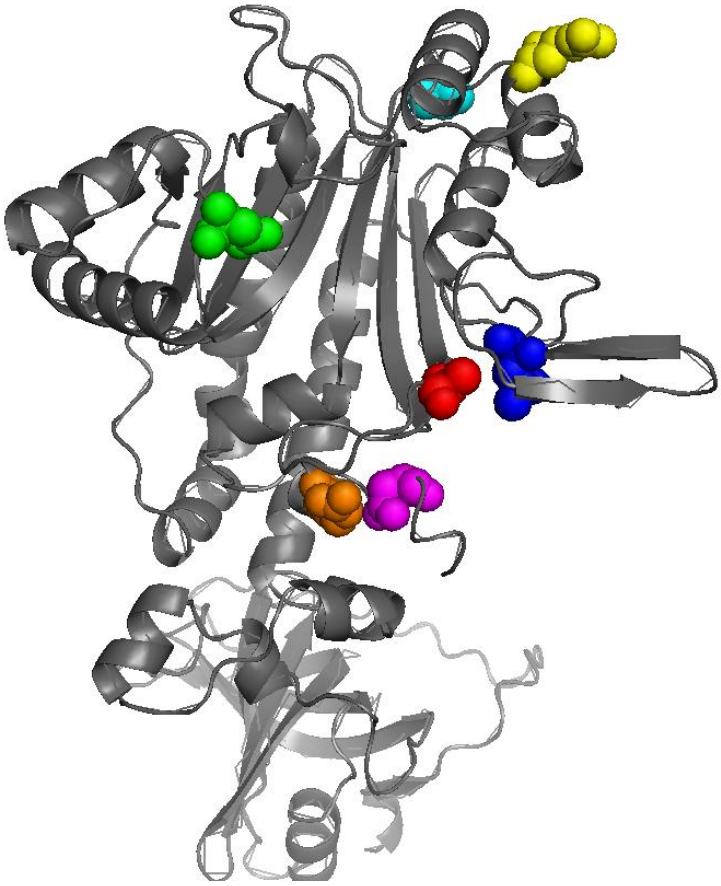

Figure S1. HBSL Mutations Mapped to the Predicted Human DARS Protein Structure

The predicted DARS protein structure (A8K3J2) was obtained from MODBASE (http://modbase.compbio.ucsf.edu/)[1]. Amino acid Met246 is shown in blue, Ala274 is shown in red, Asp367 in green, Arg460 in yellow, Pro464 in cyan, Arg487 in orange and Arg494 in magenta (see Table 1 and S4 for additional information). Note that all mutations lie within or adjacent to the active-site pocket (top center).

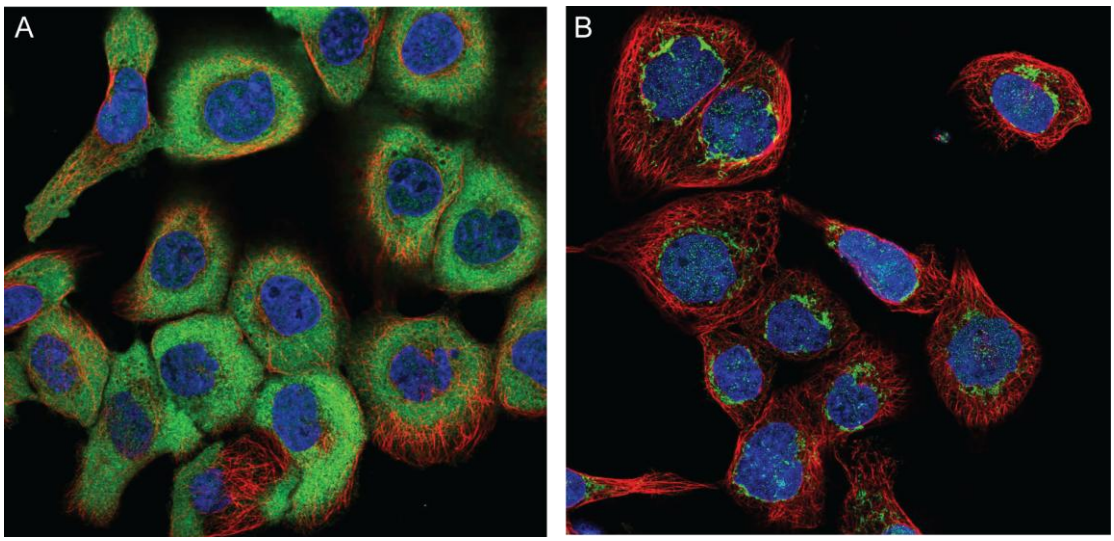

Figure S2. Subcellular Localization of *DARS* and *DARS2*

Images extracted from the Human Protein Atlas[3]. In both images nuclei are labelled in blue and microtubules in red.

(A) *DARS* expression (green, antibody HPA020451) is diffusely cytoplasmic in A-431 cells.

(B) *DARS2* expression is specific, as predicted, to mitochondria - shown here as a perinuclear green (antibody HPA026528) staining.

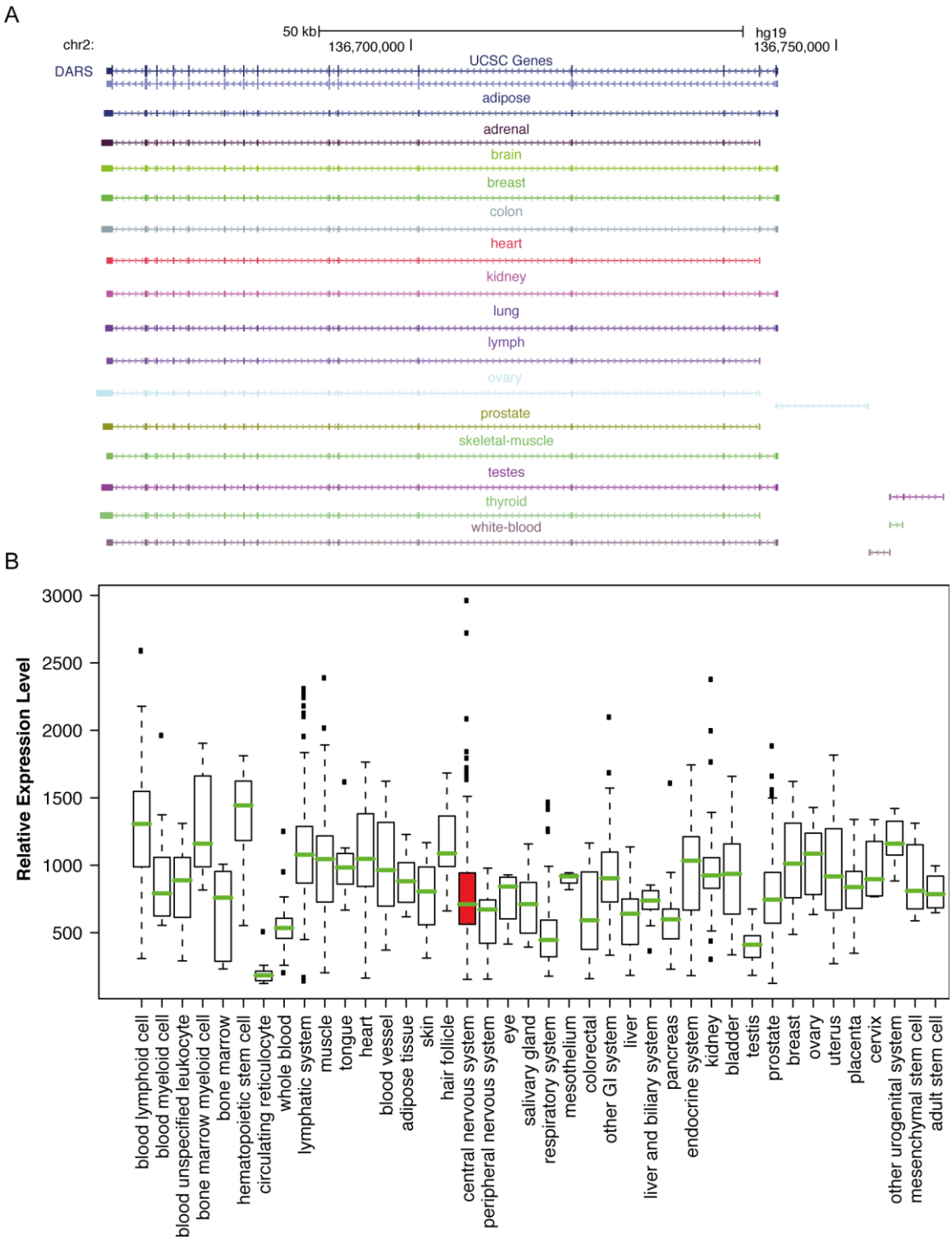

Figure S3. *DARS* Gene Expression across Human Tissues

(A) UCSC screen shot of Illumina Body Map 2 de-novo assembled *DARS* transcripts from the data generated using the Tophat/Cufflinks[2] suite, which shows that *DARS* is widely expressed in normal human tissues.

(B) *DARS* expression across 43 normal tissues (data extracted from genesapiens.org, a compilation of more than two thousand experiments on 5 different Affymetrix platforms). Expression in the central nervous system (red) shows the greatest range.

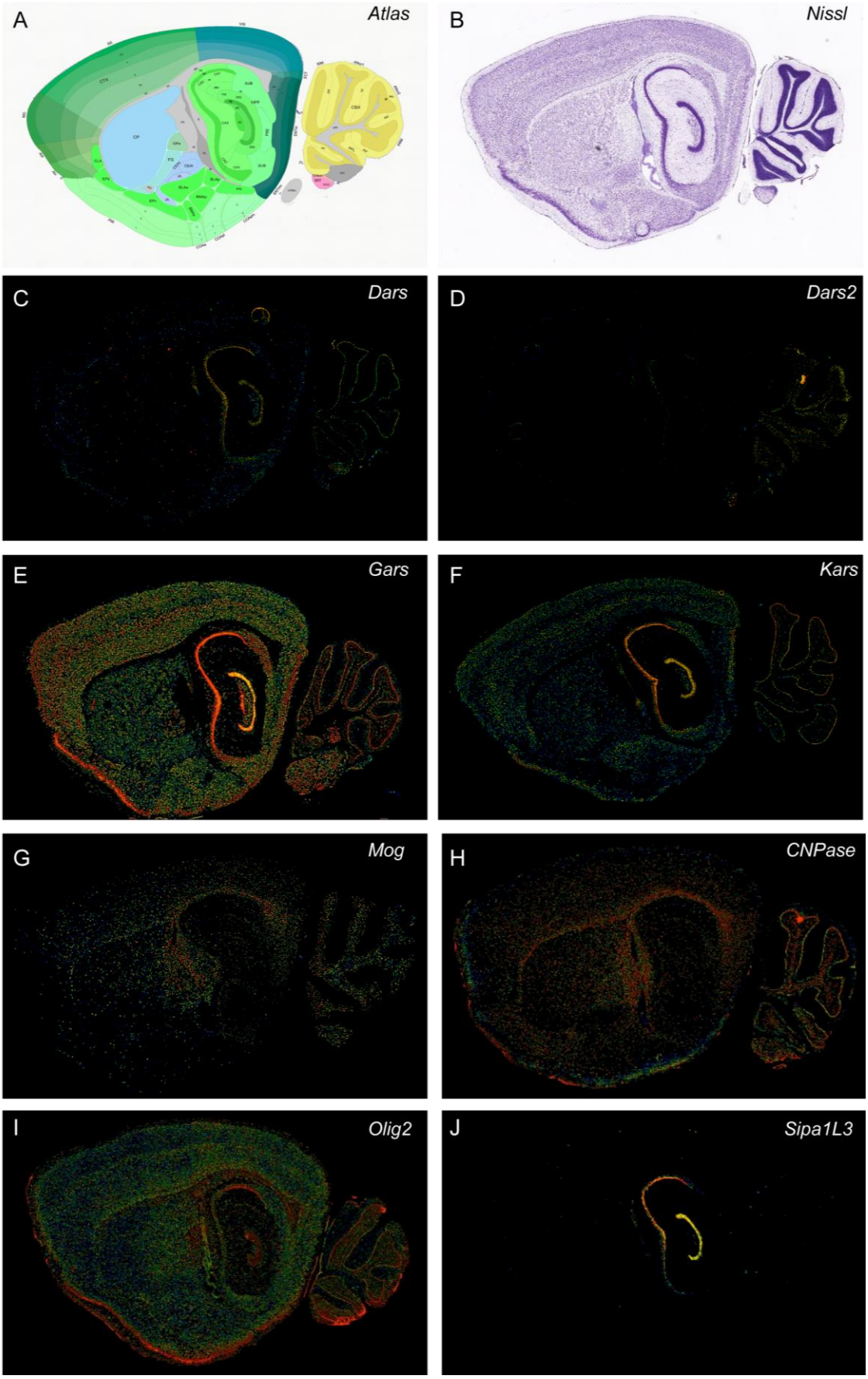

Figure S4. ***(See following page for figure legend)***

Figure S4. Region-Specific Expression of *Dars* and Other Associated Genes in Mouse Brain Sagittal Sections

All images were extracted from the Allen Mouse Brain Atlas (http://mouse.brain-map.org/), and show a sagittal false color expression image based on an in-situ hybridization signal. A full description of the data, including deconvolution of the codes given in (A) is given in AllenReferenceAtlas_v2_2011.pdf which is available at http://help.brain-map.org. Note that in each panel the CA1, CA2 and CA3 hippocampal fields are clearly visible, along with the dentate gyrus (DG), caudoputamen (CP), cerebral cortex (CTX), and cerebellar cortex (CBX) in which both the granular and molecular layer are discernable.

(A) Reference Atlas image of this sagittal plane.

(B) Nissl staining, revealing neuronal structures.

(C–F) False color expression images of four tRNA synethetases – *Dars* (cytoplasmic aspartyl-tRNA synthetase), *Dars2* (mitochondrial aspartyl tRNA-synthetase), *Gars* (gylcyl-tRNA synthetase), and *Kars* (lysl-tRNA synthetase). Note that *Dars*, *Gars* and *Kars* show high levels of expression in the hippocampus and in the molecular (but not granular) layer of the cerebellum, suggesting that tRNA synthetases may be preferentially expressed in neurons.

(G–I) False color images of three markers of oligodendrocytes - Mog, CNPase, and oligdendrocyte-specific transcription factor Olig2. Note that these expression patterns largely do not overlap with the tRNA-synthetase expression patterns, and are instead pronounced in the fiber tracts and cerebellar granular layer.

(J) Hippocampus-specific expression of neuronal marker Sipa1L3.

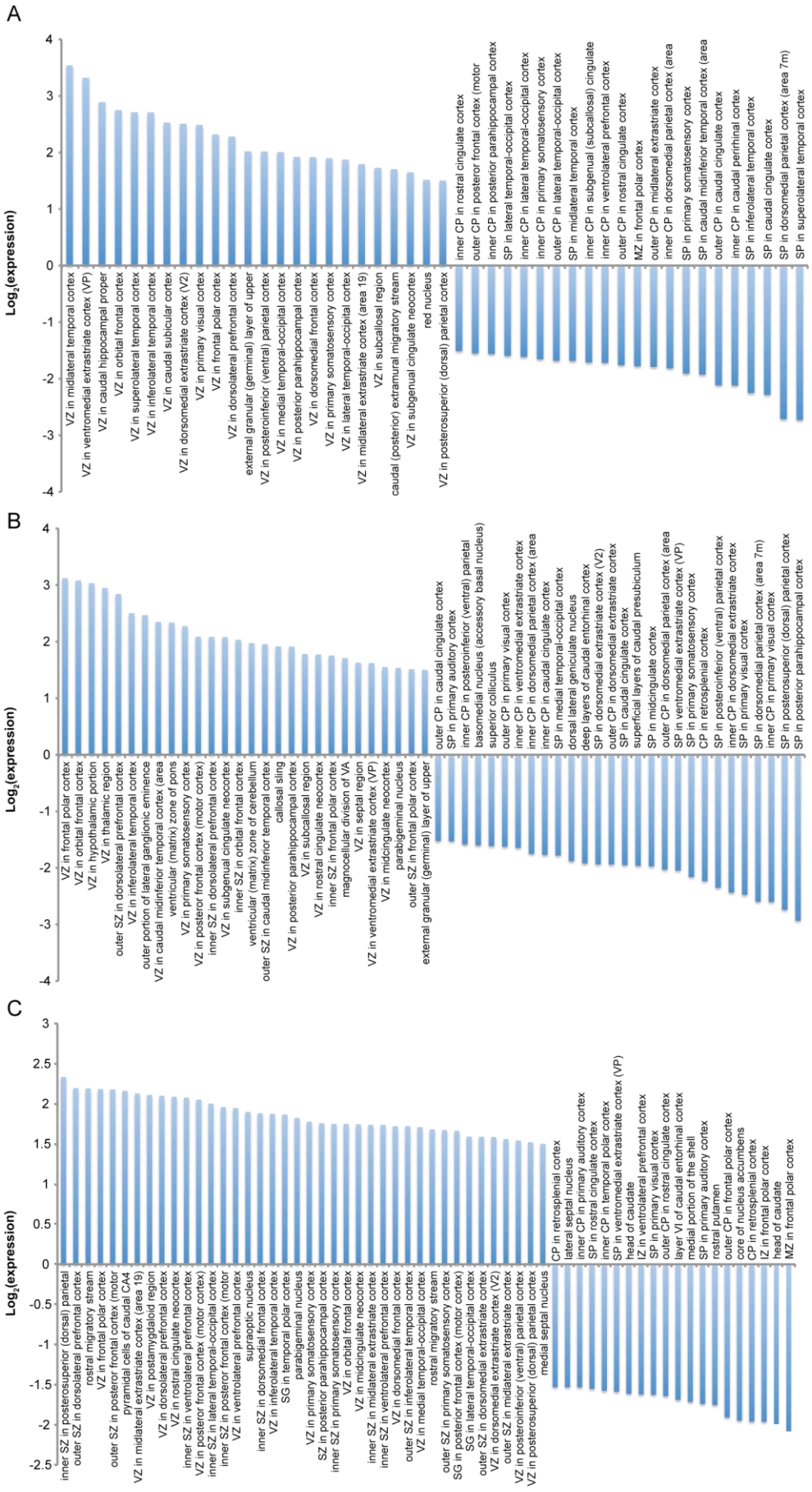

Figure S5. ***(See following page for figure legend)***

Figure S5. *DARS* Expression in the Developing Human Brain

Data for all panels were mined from the Allen Institute for Brain Science's Atlas of the Developing Human Brain (http://www.brainspan.org/). Pre-normalized expression values were extracted, and brain regions with expression levels greater than $\log_2(1.5)$ or less than $-\log_2(1.5)$ compared to the normalized average were plotted. Values shown in (A–C) are from 15 post-conception weeks (pcw), 16 pcw, or 21 pcw brains, respectively. In all three timepoints the highest expression levels are seen in structures in the ventricular and subventricular zone. Consistent with *Dars* expression in mouse brain (see Figure S4, above), hippocampal structures show high levels of DARS expression. DARS expression is also high in the midlateral temporal cortex (15 pcw), the frontal polar cortex (16 pcw), and the rostral migratory stream (a chain of immature neurons) and pyramidal cells of the caudal CA4 (21 pcw).

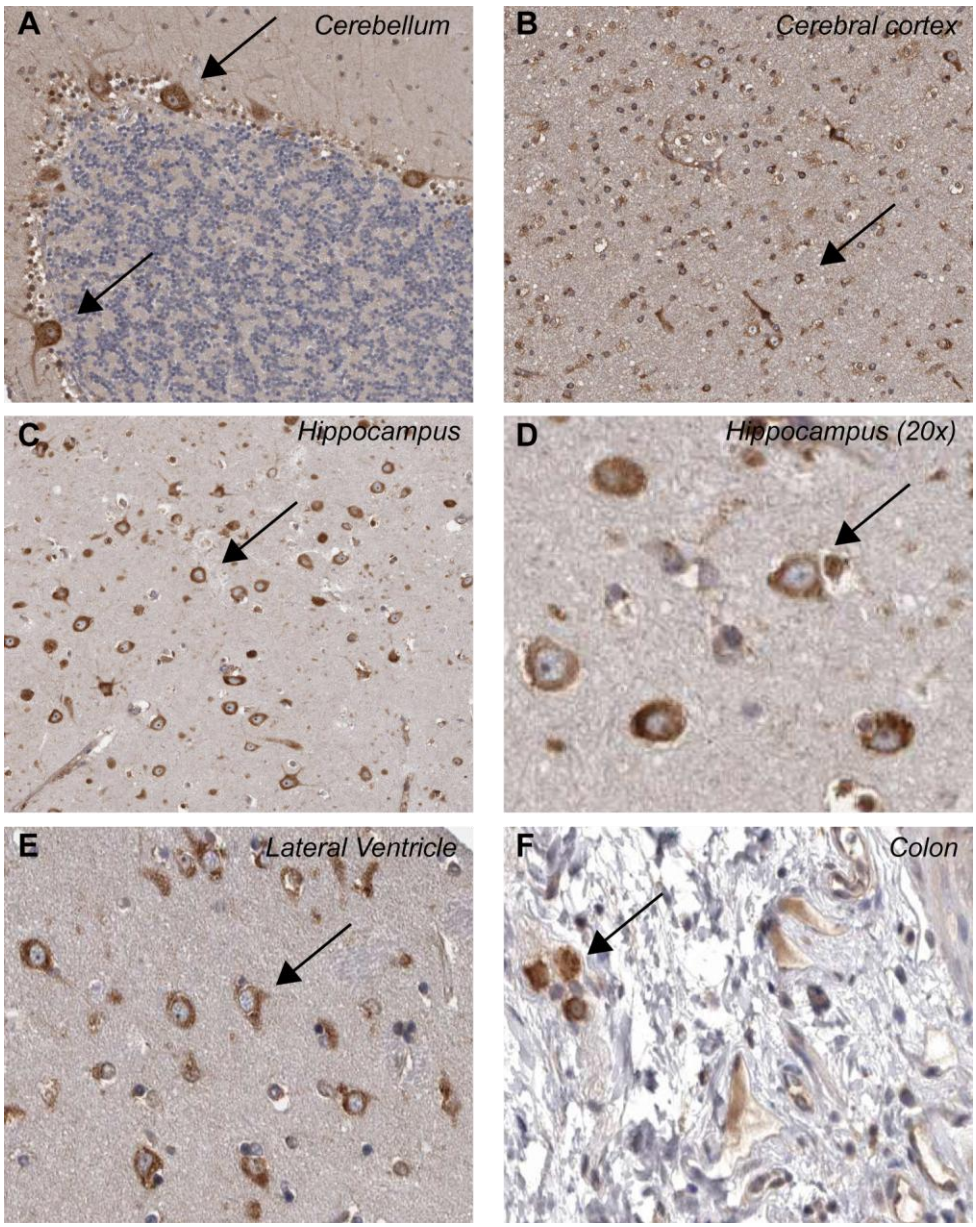

Figure S6. DARS Staining in Primary Human Tissues

All images were extracted from the Human Protein Atlas (http://www.proteinatlas.org/)[3]. Antibody HPA029804 was used for all experiments. Black arrows indicate areas of high DARS staining, all of which correspond to neurons.

(A) DARS staining in the cerebellum is pronounced in Purkinje neurons.

(B–E) DARS staining in the cerebral cortex, hippocampus and lateral ventricle is pronounced in neuronal cells.

(F) DARS staining in colon is specific to glandular cells (not shown) and peripheral neurons.

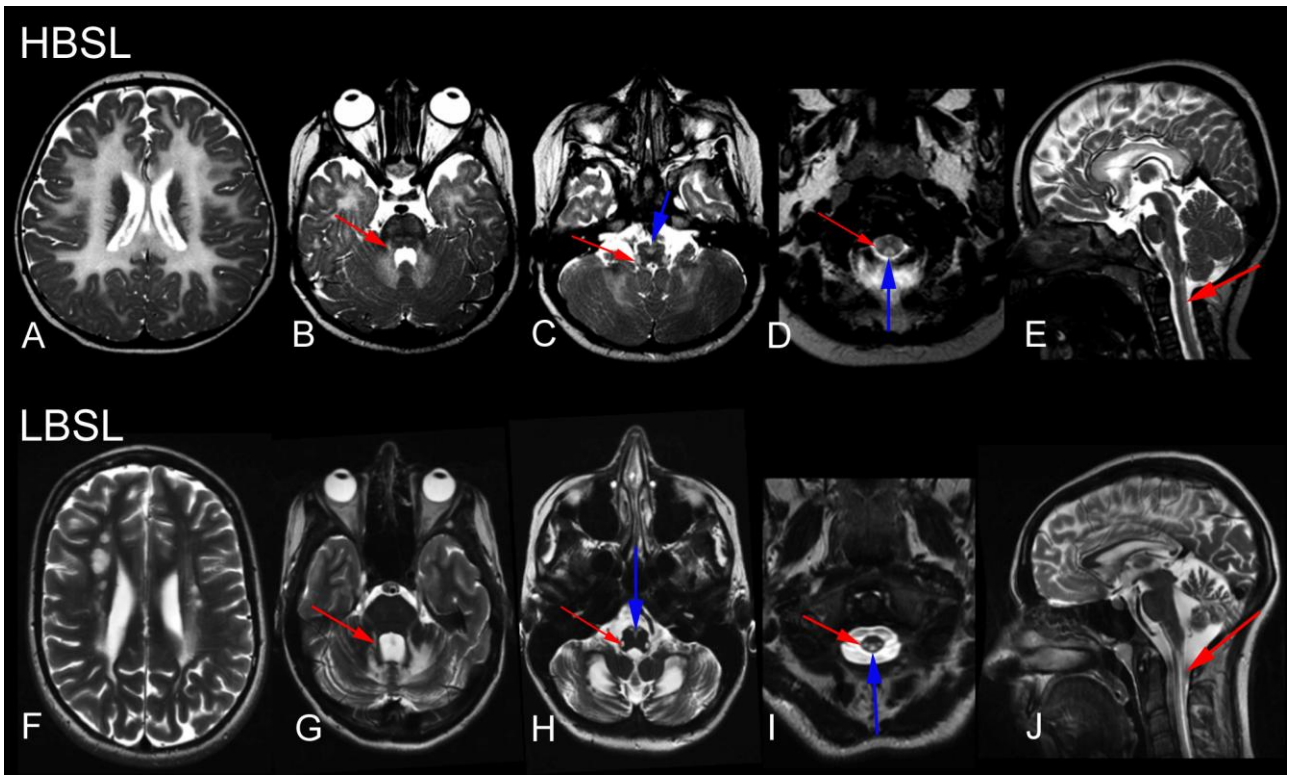

Figure S7. A Comparison of HBSL and LBSL MRI Patterns

T2-weighted MRI of a patient with HBSL (A–E) and LBSL (F–J). In the supratentorial white matter, the signal changes are homogeneous in the patient with HBSL and multifocal in the LBSL patient. Both LBSL and HBSL patients show abnormal superior cerebellar peduncles (red arrow in B and G), inferior cerebellar peduncles (red arrow in C and H), pyramidal tracts (blue arrow in C and H), lateral corticospinal tracts (red arrow in D and I) and dorsal columns (blue arrow in D and I, red arrow in E and J).

Table S1. Clinical Findings

	Subject 1	Subject 2	Subject 3	Subject 4	Subject 5	Subject 6	Subject 7	Subject 8	Subject 9	Subject 10
Patient and family characteristics										
Gender	m	m	m	m	m	f	f	m	m	f
Year of birth	2008	2006	2010	2004	2006	2001	2006	2009	2001	2001
Siblings (affected/unaffected/ otherwise affected)	0/0/0	1/0/0	1/0/0	0/1/0	0/0/0	1/1/0	1/1/0	0/0/0	1/0/0	1/0/0
Consanguinity	no	yes	yes	yes	yes	no	no	yes	no	no
Pregnancy/delivery/perinatal period	spina bifida occulta, tethered cord, solitary kidney	normal	normal	elective Caesarean section	normal	mild hyperbilirubinemia	mild hyperbiliru-binemia, episode of apnea diagnosed as gastroeosophageal reflux	vacuum-assisted delivery	elective Caesearean section	elective Caesarean section
Early motor development	normal	normal	normal	normal	developmental delay	normal	normal	normal	developmental delay	developmental delay
Early cognitive development	normal	normal	normal	normal	normal	normal	normal	normal	normal	normal
Unsupported walking (years)	never	never	never	never	never	never	never	never	never	never
Presentation										
Age at presentation	11 m	9 m	7 m	4 m	6 m	9 m	12-14 m	9 m	6m	6m
Signs at presentation	axial hypotonia, hypertonia legs>>arms	spastic diplegia, squint, nystagmus, head bobbing	ankle tightness, nystagmus, head bobbing	delayed motor development, muscle hypotonia	delayed motor development, nystagmus	abrupt loss in motor milestones after vaccination	gradual loss of motor milestones	irritable, delayed motor development	spastic diplegia	spastic diplegia
Course over time										
Further signs	progressive spasticity in legs	progressive spasticity in legs	progressive spasticity in legs	progressive spasticity, nystagmus	progressive spasticity in legs	progressive spasticity in legs	progressive spasticity in legs	progressive spasticity in legs, nystagmus	progressive spasticity in legs	progressive spasticity in legs
Regression	transient mild regression during infections	no	no	no	no	second event of regression at 12 months after urinary tract infection	slow regression after 14 months	yes	no	no
Cognition	mild mental retardation	mild mental retardation	mild mental retardation	mild mental retardation	normal	normal	normal	normal	normal	normal
Highest motor milestone	stands and cruises	walks a few steps with support, diplegic gait	sits without support	walks with support, diplegic gait	sits without support	stands and cruises	crawls and cruises	uses wheel chair, can propel a supportive walker	uses wheel chair, can propel a supportive walker	can propel a supportive walker
Epilepsy	no	no	no	yes	no	no	no	no	yes	no
ERG	n.d.	n.d.	n.d.	n.d.	n.d.	n.d.	n.d.	normal	cone dysfunction	cone dysfunction
Peripheral neuropathy	NCV normal	NCV normal	no	NCV normal	no	NCV normal	no	no	no	no
Other	very irritable					reported improvement with IVIG and steroids	reported improvement with steroids			

	Subject 1	Subject 2	Subject 3	Subject 4	Subject 5	Subject 6	Subject 7	Subject 8	Subject 9	Subject 10
Physical examination										
Age at latest examination	4 y	6 y	2 y	7 y	4 y	7 y	2 y	2 y	10 y	10 y
Head circumference	normal	< 2 SD	normal	normal	normal	< 2 SD	normal	-2 SD	normal	normal
Height	normal	normal	normal	normal	normal	< 2 SD	normal	-2 SD	normal	normal
Vision	normal	hypermetropia	normal	decreased, optic atrophy	normal	normal	normal	myopia	myopia	myopia
Extraocular eye movements	normal	nystagmus	nystagmus	nystagmus	nystagmus	normal	normal	nystagmus	nystagmus	nystagmus
Retinal abnormalities	mild optic disc pallor	no	no	no	bilateral cherry red spot	no	n.d.	pigmentary changes	optic disc pallor	optic disc pallor
Hearing	normal	normal	normal	normal	normal	normal	normal	normal	normal	Normal
Receptive language	normal	normal	normal	normal	normal	normal	normal	normal	normal	normal
Expressive language	delayed - few single words	almost age adequate	normal	speaks in sentences	normal	normal	normal	normal	normal	normal
Dysarthria	yes	yes	no	yes	no	no	no	no	no	no
Dysphagia, tube feeding	no	no	no	no	no	no	no	no	no	no
Axial tone	decreased	normal	normal	decreased	decreased	decreased	decreased	decreased	decreased	decreased
Arms										
Spasticity	no	mild	mild	mild	mild	mild	mild	no	mild	mild
Reflexes	normal	brisk	brisk	brisk	brisk	brisk	brisk	normal	brisk	brisk
Ataxia	no	yes	no	mild	could not be assessed	no	no	no	yes	mild
Extrapyramidal signs	no	no	no	no	no	dystonic posturing when reaching for objects	no	no	no	no
Legs										
Spasticity	severe	severe	severe	severe	severe	severe	severe	severe	severe	severe
Reflexes	brisk	brisk	brisk	brisk	brisk	brisk	brisk	brisk	brisk	brisk
Babinski signs	present	present	present	present	present	present	present	present	present	present
Extrapyramidal signs	no	no	no	no	no	no	no	no	no	no

n.d. not done; NCV nerve conduction velocity; IVIG intravenous immunoglobulins; SD standard deviation

Table S2. MRI Findings

	Subject 1	Subject 2	Subject 4	Subject 5	Subject 6	Subject 7	Subject 8	Subject 9	Subject 10
Age at MRI	3 y	5 y	8 y	4 y	6 y	2 y	24 m	8 y	20 m
Signal of supratentorial white matter									
Homogeneously abnormal	+	+	+	+	+	+	+	+	+
Consistent with hypomyelination	-	-	+	+	+	-	+	+	-
Subocortical T1 hyperintense rim	+	+	+	-	+	+	+	+	+
Abnormal signal of internal capsule	+*	+*	+	+	+*	+*	+	+	+*
Corpus callosum									
Hyperintensity	+	+	+	+	+	+	+	+	+
Thinning	+	+	+	+	+	-	+	+	-
Supratentorial atrophy									
Generalised	-	-	-	-	-	-	-	-	-
Brainstem									
Abnormal signal of anterior brainstem	+	+	+	+	faint	faint	faint	faint	-
Abnormal signal of pyramidal tracts	+	+	+	+	faint	-	faint	faint	-
Abnormal signal of medial lemniscus	-	-	+	-	-	-	-	-	-
Cerebellum									
Cerebellar atrophy	-	-	-	-	-	-	-	-	-
Abnormal signal of white matter	-	-	+	+**	-	-	+**	+**	-
Abnormal signal of superior cerebellar peduncles	+	+	+	+	+	+	+	+	+
Abnormal signal of inferior cerebellar peduncles	+	+	+	+	-	-	+	+	+
Spinal cord									
Abnormal signal of dorsal columns	+	+	+	+	faint	+	+	n.d.	n.d.
Abnormal signal of lateral corticospinal tracts	+	n.d.	+	+	n.d.	+	+	n.d.	n.d.
Proton MRS									
lactate elevated	n.d.	n.d.	-	n.d.	-	n.d.	-	n.d.	n.d.

*anterior aspect of posterior limb has normal signal; **around the dentate nucleus; n.d. - not done

Table S3. Genome and Exome Coverage Statistics

Family	Individual	Affected	Mapped Sequence (Gb)	Genome or Exome Target Bases		
				Mean Depth	Q20 Depth	Percent > 18x[b]
1[a]	Subject 1	Yes	140.8	45.35	41	90
	Mother	No	122.4	39.5	37	86.6
	Father	No	126.8	40.9	37.4	87.2
2	Subject 2	Yes	10.2	68.1	67.6	96.6
	Mother	No	6.3	45.8	45.4	90.9
3	Subject 4	Yes	11.0	80.7	80.2	97.4
6	Subject 6	Yes	36.4	133	127	96.4
	Subject 7	Yes	37.5	57.1	56.1	93.6
	Sibling	No	23.3	75.1	73.7	93.4
	Mother	No	19.3	92.5	87.9	94.7
	Father	No	36.1	119	114	96.1

[a] For family 1, whole genome sequencing data is presented. Whole genome sequencing of Subject 1 was performed at Illumina (San Diego, CA) on eight GAIIx flow cells. Sequencing of this the parental DNA samples was performed at Macrogen (South Korea) on a HiSeq200 yielding in excess of 120 Gb of mappable sequencing reads. All other data presented here is whole exome sequencing performed at one of two sites – the Queensland Centre for Medical Genomics at the University of Queensland or the Department of Medical Genetics, VU University Medical Center. In both cases, DNA was isolated from peripheral blood and was sheared with a Covaris S2 Ultrasonicator. An adaptor-ligated library was prepared with the Paired-End Sample Prep kit V1 (Illumina). Exome capture was performed with the SeqCap EZ Exome Library v2.0 (Subject 2 and mother, and Subject 4) or v3.0 (Subject 6, 7 and their family members). 100 bp paired-end sequencing was carried out on an Illumina HiSeq 2000.

[b] Percentage of target bases (i.e. the whole genome or exome caputured regions) covered by a minimum of 18 reads.

Table S4. *DARS* Mutation Damage Prediction*

Genomic Position	cDNA	Amino Acid	Inheritance State	SIFT	Pmut	PolyPhen-2	GVGD	MutationTaster	Mutpred P_{del}
chr2:136680399	c.766A>C	Met256Leu	Homozygous (x4)	0.02 Not tolerated	Neutral	0.92	Class C0	Disease causing	0.55
chr2:136678161	c.821C>T	Ala274Val	Compound het with Asp367Tyr (x1)	0.00 Not tolerated	Pathogenic	1.00	Class C65	Disease causing	0.963
chr2:136673803	c.1099G>T	Asp367Tyr	Compound het with Ala274Val (x1)	0.00 Not tolerated	Neutral	0.99	Class C65	Disease causing	0.685
chr2:136668733	c.1391C>T	Pro464Leu	Compound het with Arg494Cys (x1)	0.00 Not tolerated	Pathogenic	1.00	Class C65	Disease causing	0.735
chr2:136668744	c.1379G>A	Arg460His	Compound het with Arg494Gly (x1)	0.06 Tolerated	Pathogenic	1.00	Class C25	Disease causing	0.61
chr2:136664933	c.1459C>T	Arg487Cys	Homozygous (x1)	0.00 Not tolerated	Pathogenic	1.00	Class C65	Disease causing	0.953
chr2:136664912	c.1480C>T	Arg494Cys	Compound het with Pro464Leu (x1)	0.00 Not tolerated	Pathogenic	1.00	Class C65	Disease causing	0.856
chr2:136664912	c.1480C>G	Arg494Gly	Compound het with Arg460His (x1)	0.00 Not tolerated	Pathogenic	1.00	Class C65	Disease causing	0.89

*All variants were initially annotated using an in-house custom software package that allows for dynamic sorting and isolation of potential pathogenic variants. Subsequent analysis was performed using an in-house screen for variant pathogenicity, which selectively parses variants through SIFT (http://sift.bii.a-star.edu.sg/)[4], Pmut (http://mmb.pcb.ub.es/PMut/), PolyPhen2 (http://genetics.bwh.harvard.edu/pph2/)[5], GVGD (http://agvgd.iarc.fr/)[6], MutationTaster (http://mutationtaster.org)[7], and MutPred (http://mutpred.mutdb.org/)[8].

Table S5. Effect of Aspartyl-tRNA Transferase Loss in Model Organisms

Method	Phenotype/Outcome	Ref
D. melanogaster		
Transgenic RNAi	Systematic neuroblast screen revealed RNAi knockdown of Aats-asp showed shorter lineages, alterations to neuroblast shape, alterations ganglion mother cell shape, and increases in the size of number of GFP aggregates associated with the cell membrane (UAS-CD8::GFp).	[9]
Genetic deletion	Embyronic lethal	[10]
Transgenic RNAi	Lethal during pupal development	[11]
S. cerevisae		
Gene deletion mutant	Inviable	[12]
Native promoter replacement with a $TetO_7$ cassette	Accumulation of cells with a 1C DNA content, indicative of a G1 arrest or delay.	[13]
Site-specific insertions and deletions	Mutations in the N-terminal domain are not damaging. C-terminal mutations result in a minimum 3-fold reduction, to a maximum of complete elimination of enzyme activity. Severe reduction or elimination of DPS1 leads to inviability.	[14]
Site-specific mutagenesis.	Any alteration to the hydrogen bond network that supports the active site leads to complete ablation of enzyme activity.	[15]
Overexpression	Slow vegetative growth	[16]

References

1. Pieper, U., Webb, B.M., Barkan, D.T., Schneidman-Duhovny, D., Schlessinger, A., Braberg, H., Yang, Z., Meng, E.C., Pettersen, E.F., Huang, C.C., et al. (2011). ModBase, a database of annotated comparative protein structure models, and associated resources. Nucleic Acids Research *39*, D465–D474.

2. Trapnell, C., Roberts, A., Goff, L., Pertea, G., Kim, D., Kelley, D.R., Pimentel, H., Salzberg, S.L., Rinn, J.L., and Pachter, L. (2012). Differential gene and transcript expression analysis of RNA-seq experiments with TopHat and Cufflinks. Unknown *7*, 562–578.

3. Uhlen, M., Oksvold, P., Fagerberg, L., Lundberg, E., Jonasson, K., Forsberg, M., Zwahlen, M., Kampf, C., Wester, K., Hober, S., et al. (2010). Towards a knowledge-based Human Protein Atlas. Nat Biotechnol *28*, 1248–1250.

4. Kumar, P., Henikoff, S., and Ng, P.C. (2009). Predicting the effects of coding non-synonymous variants on protein function using the SIFT algorithm. Unknown *4*, 1073–1081.

5. Adzhubei, I.A., Schmidt, S., Peshkin, L., Ramensky, V.E., Gerasimova, A., Bork, P., Kondrashov, A.S., and Sunyaev, S.R. (2010). A method and server for predicting damaging missense mutations. Nat Meth *7*, 248–249.

6. Mathe, E., Olivier, M., Kato, S., Ishioka, C., Hainaut, P., and Tavtigian, S.V. (2006). Computational approaches for predicting the biological effect of p53 missense mutations: a comparison of three sequence analysis based methods. Nucleic Acids Research *34*, 1317–1325.

7. Schwarz, J.M., Rödelsperger, C., Schuelke, M., and Seelow, D. (2010). MutationTaster evaluates disease-causing potential of sequence alterations. Nat Meth *7*, 575–576.

8. Li, B., Krishnan, V.G., Mort, M.E., Xin, F., Kamati, K.K., Cooper, D.N., Mooney, S.D., and Radivojac, P. (2009). Automated inference of molecular mechanisms of disease from amino acid substitutions. Bioinformatics *25*, 2744–2750.

9. Neumüller, R.A., Richter, C., Fischer, A., Novatchkova, M., Neumüller, K.G., and Knoblich, J.A. (2011). Genome-wide analysis of self-renewal in Drosophila neural stem cells by transgenic RNAi. Cell Stem Cell *8*, 580–593.

10. Stitzinger, S.M., Pellicena-Palle, A., Albrecht, E.B., Gajewski, K.M., Beckingham, K.M., and Salz, H.K. (1999). Mutations in the predicted aspartyl tRNA synthetase of Drosophila are lethal and function as dosage-sensitive maternal modifiers of the sex determination gene Sex-lethal. Mol. Gen. Genet. *261*, 142–151.

11. Mummery-Widmer, J.L., Yamazaki, M., Stoeger, T., Novatchkova, M., Bhalerao, S., Chen, D., Dietzl, G., Dickson, B.J., and Knoblich, J.A. (2009). Genome-wide analysis of Notch signalling in Drosophila by transgenic RNAi. Nature *458*, 987–992.

12. Giaever, G., Chu, A.M., Ni, L., Connelly, C., Riles, L., Véronneau, S., Dow, S., Lucau-Danila, A., Anderson, K., André, B., et al. (2002). Functional profiling of the Saccharomyces cerevisiae genome. Nature *418*, 387–391.

13. Yu, L., Peña Castillo, L., Mnaimneh, S., Hughes, T.R., and Brown, G.W. (2006). A survey of essential gene function in the yeast cell division cycle. Mol Biol Cell *17*, 4736–4747.

14. Prevost, G., Eriani, G., Kern, D., Dirheimer, G., and Gangloff, J. (1989). Study of the arrangement of the functional domains along the yeast cytoplasmic aspartyl-tRNA synthetase. Eur J Biochem *180*, 351–358.

15. Cavarelli, J., Eriani, G., Rees, B., Ruff, M., Boeglin, M., Mitschler, A., Martin, F., Gangloff, J., Thierry, J.C., and Moras, D. (1994). The active site of yeast aspartyl-tRNA synthetase: structural and functional aspects of the aminoacylation reaction. Embo J *13*, 327–337.

16. Yoshikawa, K., Tanaka, T., Ida, Y., Furusawa, C., Hirasawa, T., and Shimizu, H. (2011). Comprehensive phenotypic analysis of single-gene deletion and overexpression strains of Saccharomyces cerevisiae. Yeast *28*, 349–361.